Electronic Supporting Information

Chemically doped perylene diimide lamellae based field effect transistor with low operating voltage and high charge carrier mobility

Arulraj Arulkashmir, Bhanprakash Jain, Jino C. John, Kanak Roy and Kothandam Krishnamoorthy*

*Synthesis of N, N'-Di-(phenyl-3, 5-dicarboxylic acid)-perylene-3,4,9,10-tetracarboxylic acid diimide ligand (**1**):*

A mixture of 0.500g (1.274 mmol) of 3,4,9,10-perylene tetracarboxylic dianhydride, 0.694g (3.823 mmol) of 5-amino isophthalic acid, 20 g of imidazole and 0.100 g (0.456 mmol) of zinc acetate was heated at 140^{o}C for 20 h under argon atmosphere. Mixture was cooled and 100ml of 2N hydrochloric acid was added for precipitation of product. The precipitate was collected by vacuum filtration and washed with a mixture of methanol and water. The product **1** was dried at 100^{o}C for 12 h.[1]

^{1}H NMR of 1 (400 MHz , D2O,25^{0}C) δ (ppm) = 8.43 (s,2H), 8.35 (s,4H), 8.02 (m,8H), MALDI-TOF (m/z): m/z calc. for $C_{40}H_{18}N_2O_{12}$ 718.59, found 719.05, [2,5-dihydroxy benzoic acid (DHB) matrix]. IR (KBr) νmax = 743, 808, 851, 1118, 1251, 1353, 1573, 1596, 1664, 1698, 2974, 3154, 3410 cm^{-1}.

*Complexation of ligand with Zn(II) ion (**2**):*

Zinc nitrate hexahydrate (0.087 g, 0.291 mmol) and 1 (0.060 g, 0.081 mmol) were dissolved in DMF/1,4-Dioxane/H_2O Ratio 3:1:1 in Teflon liner. The reaction mixture was heated in oven at 100 °C for 3 Days. The reaction vessel was then removed from the oven and allowed to cool to room temperature. Product was washed with DMF, methanol and chloroform.[2] IR spectroscopy was used to confirm the coordination of zinc with the carboxylic acid moieties of **1**. The presence of stretching peaks at 1588 cm^{-1} (C=O) and 1243 cm^{-1} (C-O), which were at 1595 cm^{-1} (C=O) and 1255 cm^{-1} (C-O) in case of 1 indicates the formation of coordination

bond between zinc and carboxylic acid functionalities.[2] The disappearance of –OH (COOH moiety) stretching peak at 3410 cm^{-1} in case of **2** is a further confirmation of coordination of zinc with carboxylic acid moieties (ESI, Fig. S6). Inductively Coupled Plasma Atomic Emission Spectroscopy (ICP-AES) was used to further confirm the presence of zinc in **2**. ICP-AES is an effective and sensitive tool to quantitatively determine the presence of metals in organic compounds. The presence of 3.54 mg/l of zinc in **2**, further confirms the reaction between zinc and **1**.

Ultra Violet Photoelectron Spectroscopy Studies:

UV photoelectron spectral (UVPES) studies of perylene diimide materials were recorded with custom built ambient pressure photoelectron spectrometer (APPES) (Prevac, Poland), equipped with discharge lamp to generate different UV radiations, such as He I or He II with He (UVS 40A2 from Prevac), MX650 monochromator and VG Scienta's R3000HP analyser[5] The water cooled UV source is mounted on a CF40 flange which can give an emission current up to 100 mA for He I and 200 mA for He II. Base pressure in the analysis chamber was maintained around 2 x 10^{-10} Torr and better than 1×10^{-9} Torr during UVPES experiments. All UVPES measurements were carried out at a pass energy of 2 eV. High-resolution core level XPS spectra of different elements were also recorded with monochromatized Al Kα with MX650.

UVPES is an excellent tool to determine orbital energy levels of polymers.[6] We employed ultra violet photo electron spectroscopy to determine the effect of hydrazine doping on the frontier orbital levels of compound **1** and **2**. The HOMO and LUMO energy levels of **1** was determined to be -6 and -4 eV, respectively by cyclicvoltammetry (ESI, Fig. S13). In UVPES, the onset of HOMO photoelectron emission was observed at a binding energy (BE) of -5.9 eV for **1** and **2** (ESI, Fig. S19 a and b). Upon addition of hydrazine, the HOMO energy level shifted to lower binding energy by 0.8 (**1**) and 1 eV (**2**). Indeed, a huge increase in

HOMO electron emission intensity was observed after reduction with hydrazine (ESI, Fig. S19 a and b). The shift in HOMO to lower BE along with an increase in the electron count is likely due to the filling of electrons in the half/partially filled HOMO energy level, which was at -6 eV below the redox energy level of hydrazine (-5.2 eV). Upon electron filling this energy level is destabilised to -5.1 and -4.9 eV for **1** and **2**, respectively. Furthermore, the above HOMO destabilisation (from UVPES) could be incorporated by subtracting 1 eV from the electrochemically determined HOMO, which places the new energy level of 2 at -5 eV.

ESR Measurements:

Electron spin resonance (ESR) spectra were recorded at room temperature with a JES - FA200 ESR Spectrometer under the settings of center field, 338.0 G, microwave frequency, 9.1 GHz, power, 3.0 mW. ESR spectra of 1 and 2 free radicals were measured in DMF solutions (50 μM) with doping of hydrazine.

Device fabrication:

The Field effect transistor devices were fabricated by drop casting the DMF solution of **1** and **2** on prefabricated transistor electrodes. This is made up of heavily n-doped silicon as a gate and SiO_2 as an insulating layer (capacitance - 14nF/cm^2). Thirty nanometer thick gold source and drain electrodes were used. The length and width of the channel are 20μm and 10mm, respectively. This was purchased from Fraunhofer microelectronics institute. The electrodes were cleaned thoroughly with acetone and i-propanol and dried with hot air.[3] Then the semiconducting materials (**1** and **2**) was drop casted on device and heated at 150^{o}C to evaporate the solvents. After that on the same device 3 drops of hydrazine was added and heated at 150^{o}C before subjecting the device for I-V measurements. The SiO_2 gate oxide was not modified to provide surface -OH functionalities that would interact with the radicals of

hydrazine treated **1** and **2**. This interaction is expected to decrease the operating voltage and sub threshold slope.[4] The charge carrier mobility was calculated from the saturation regime.[7]

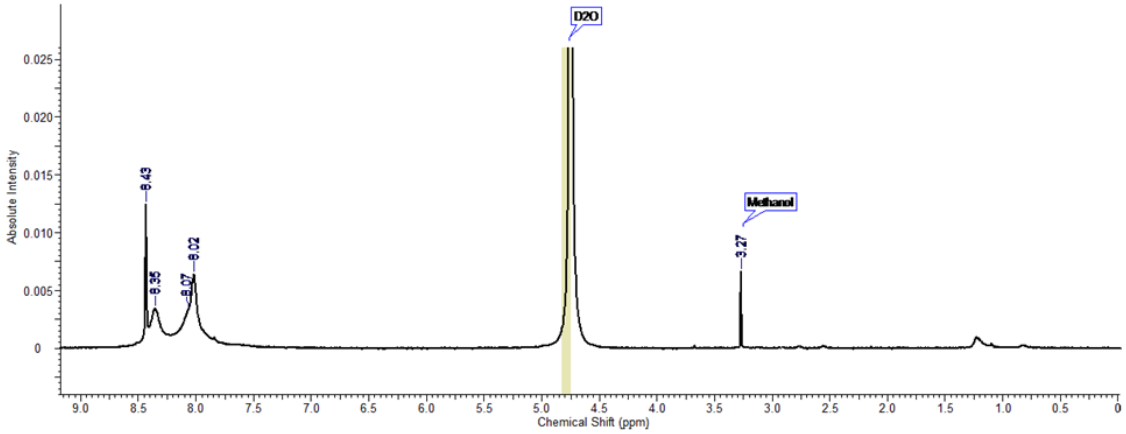

Fig. S1. ^{1}H NMR (400 MHz, D_2O) Spectrum of compound **1.**

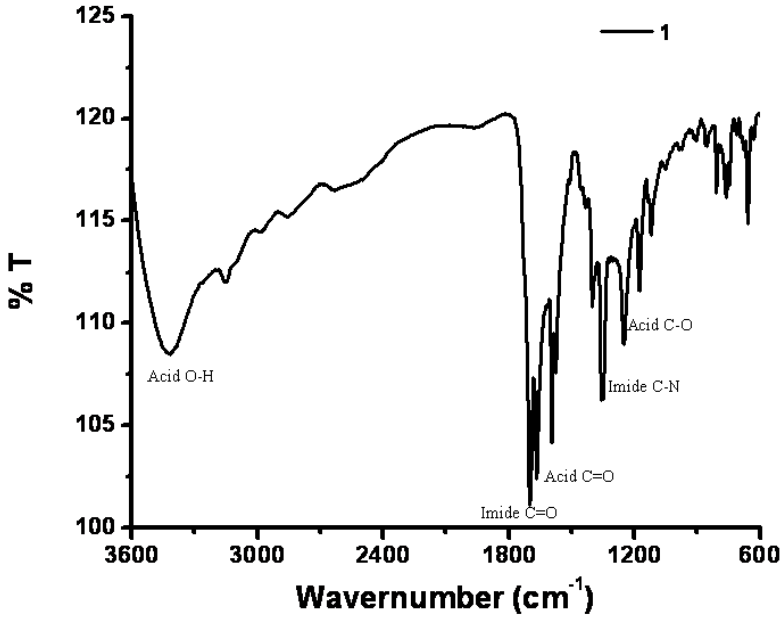

Fig. S2. Fourier transform Infrared (FT-IR) spectrum of compound **1.**

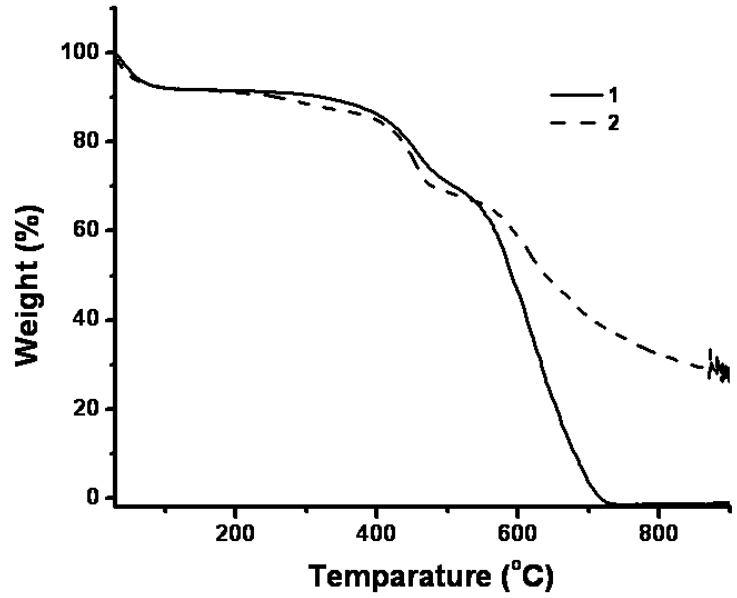

Fig. S3. Thermo gravimetric curve for **1** and **2.**

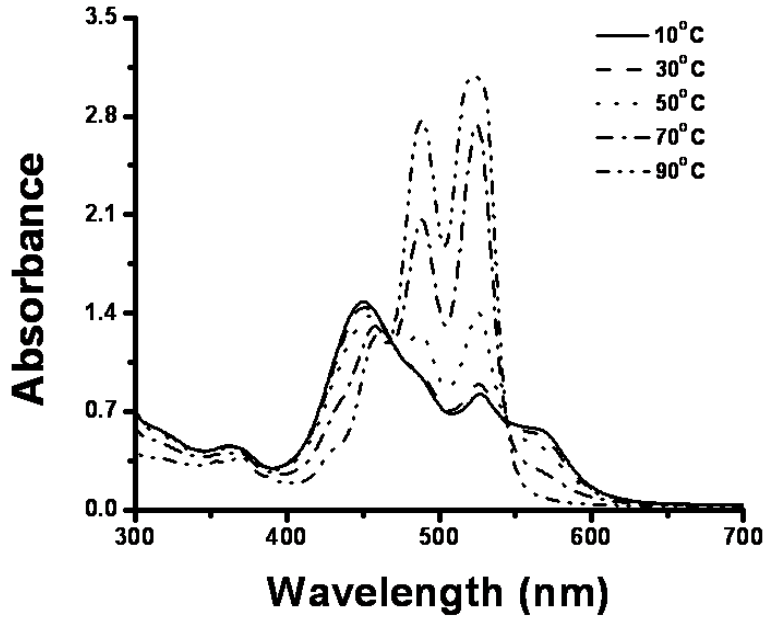

Fig. S4. UV-visible absorption spectra of compound **1** as a function of temperature.

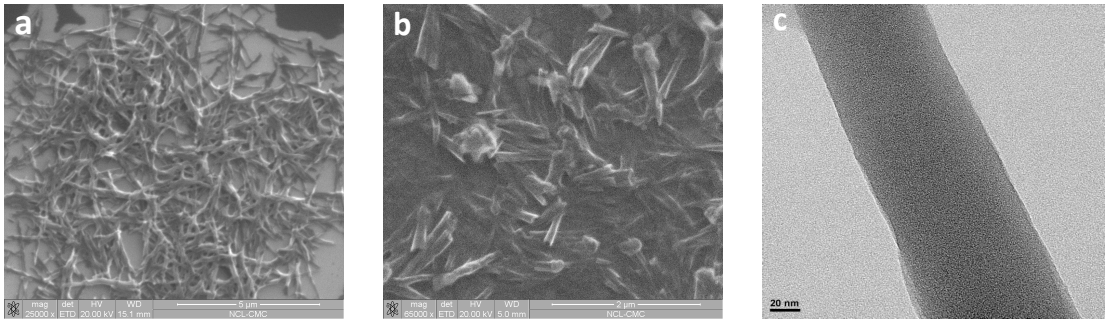

Fig. S5. Scanning Electron Microscopic (SEM) images of **1** before (a) and after (b) hydrazine reduction**.** (c) HRTEM image of **1.**

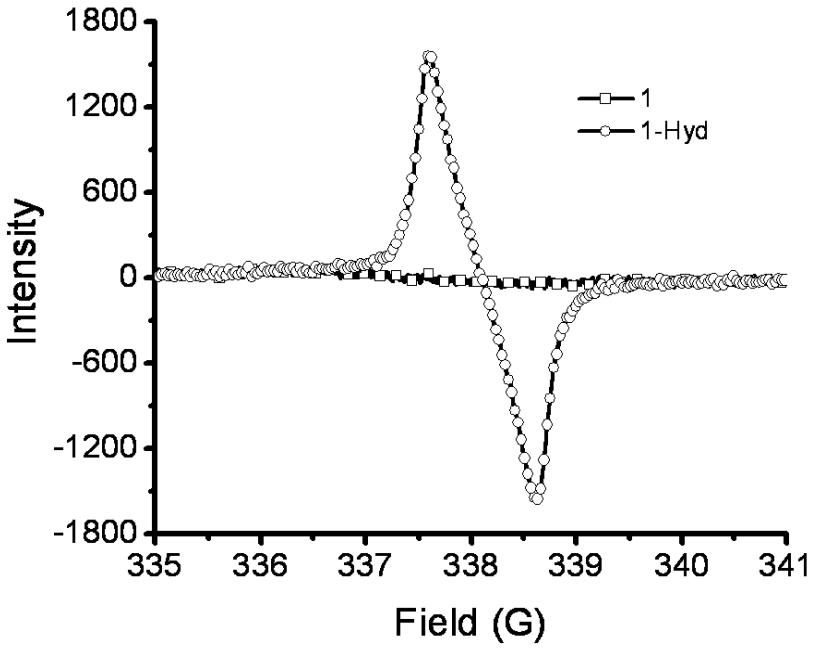

Fig. S6. Electron paramagnetic resonance (EPR) spectra for compound **1** (with and without hydrazine doping)**.**

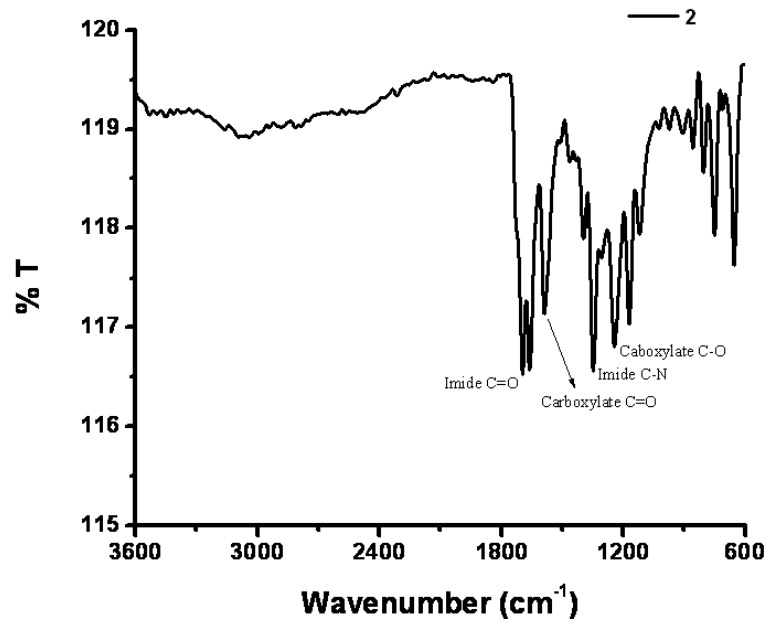

Fig. S7. Fourier transform Infrared (FT-IR) spectrum of compound **2.**

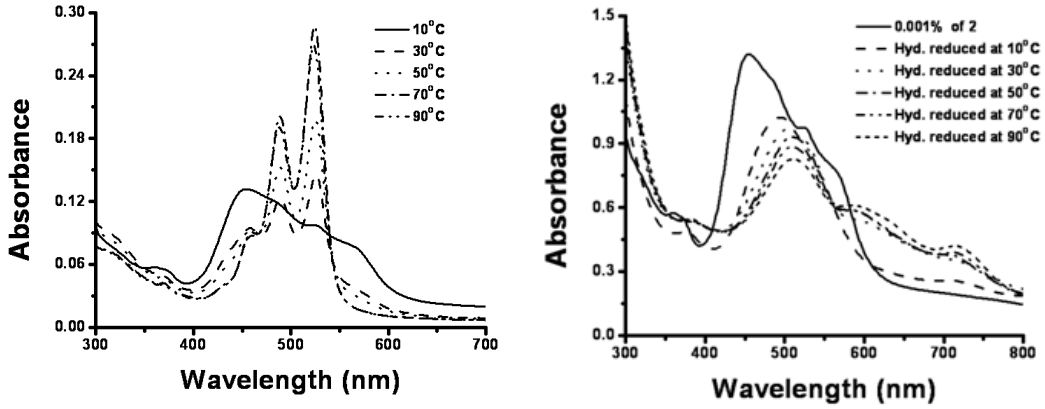

Fig. S8. UV vis absorption spectra of compound **2** as a function of temperature (left). UV-vis absorption spectra of **2** as a function of temperature upon hydrazine addition (right).

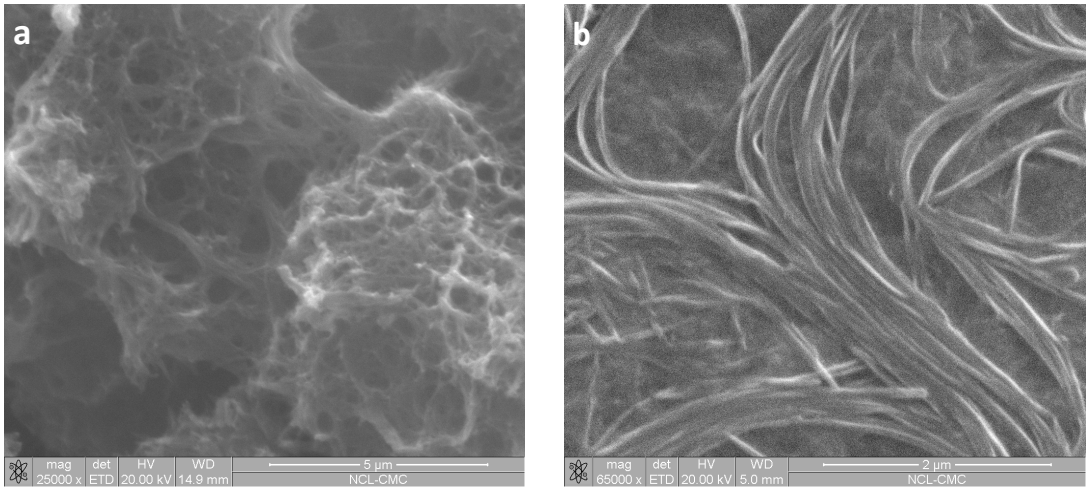

Fig. S9. Scanning Electron Microscopic (SEM) images of **2** before (a) and after (b) hydrazine reduction**.**

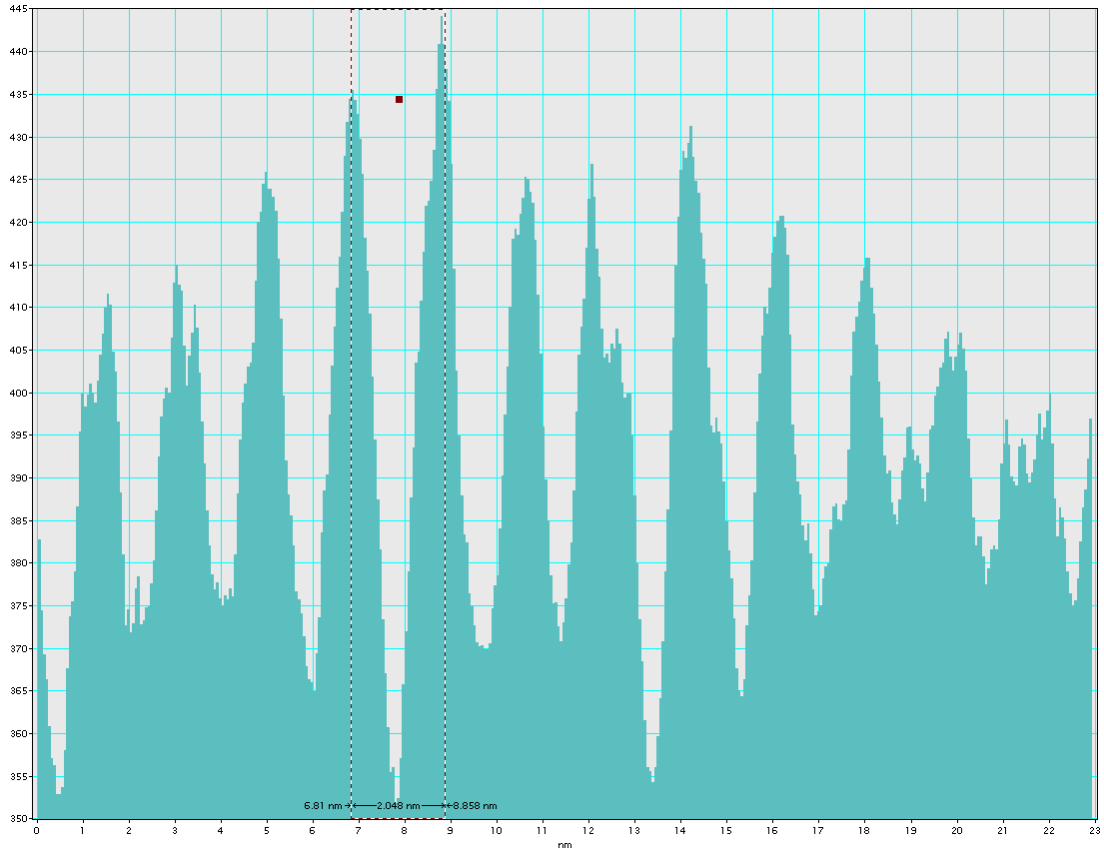

Fig. S10. Lattice fringes showing the individual lamella spacing of ~ 2nm (calculated for the image in Fig. 2c)

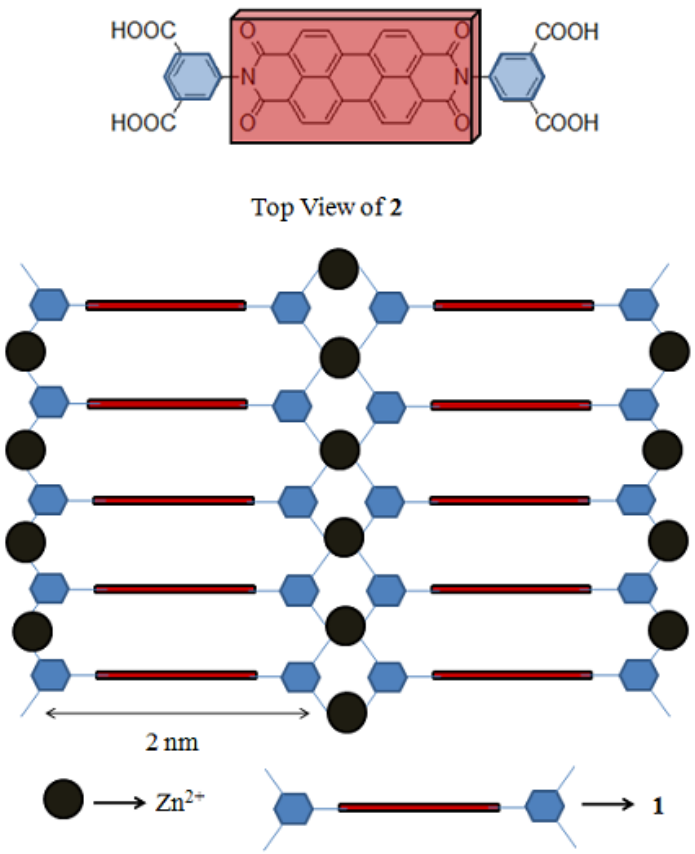

Fig. S11. Cartoon showing the plausible mode of binding between Zn^{2+} and compound 1 to form lamellar assembly.

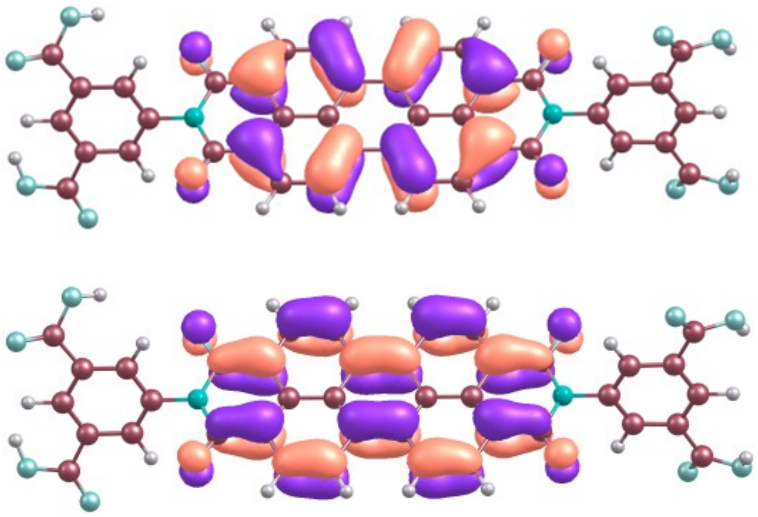

Fig. S12. HOMO (top) and LUMO (bottom) orbital diagram of compound 1 (length of the molecule is ~ 2.2nm).

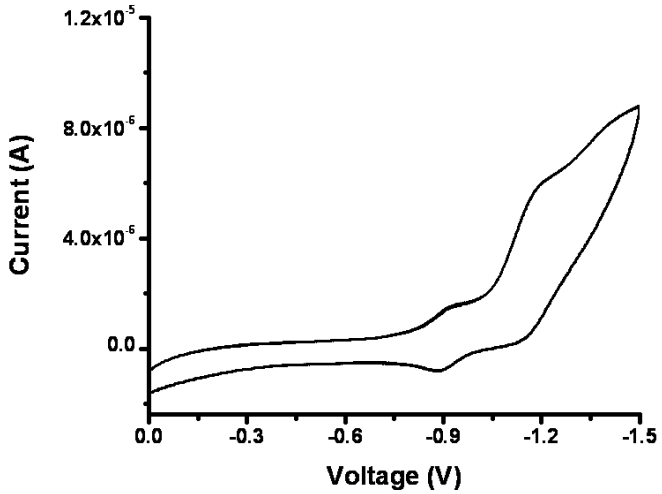

Fig. S13. Cyclic voltammogram of **1** in DMF with 0.1 M tetra butyl ammonium hexafluoro phosphate (supporting electrolyte)**.**

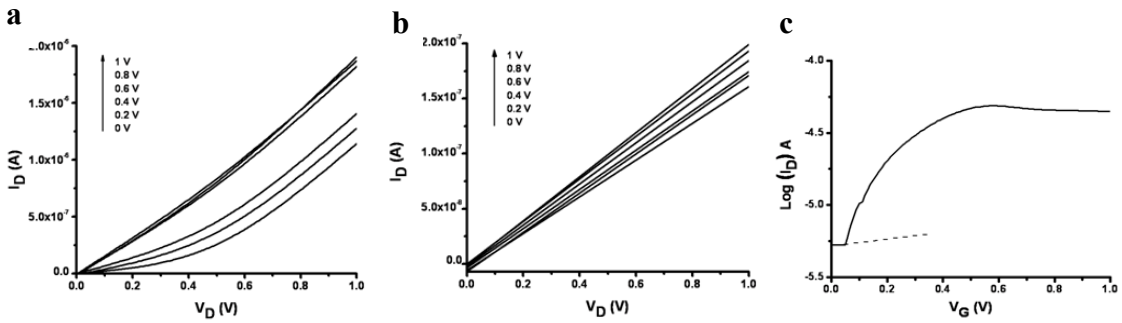

Fig. S14. a) Output characteristic IV curves of 2. b) Output characteristic IV curve of hydrazine doped 2 after 240 h of exposure to ambient conditions. c) The plot showing the calculation of sub threshold slope for hydrazine doped 2.

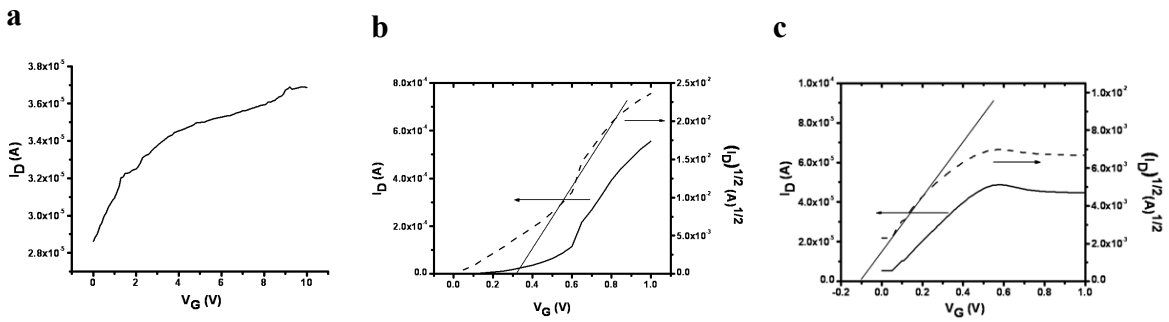

Fig. S15. a) Transfer Characteristics of compound **1** and b) **2** before hydrazine doping**,** and transfer curves for compound **2** with hydrazine doping (c).

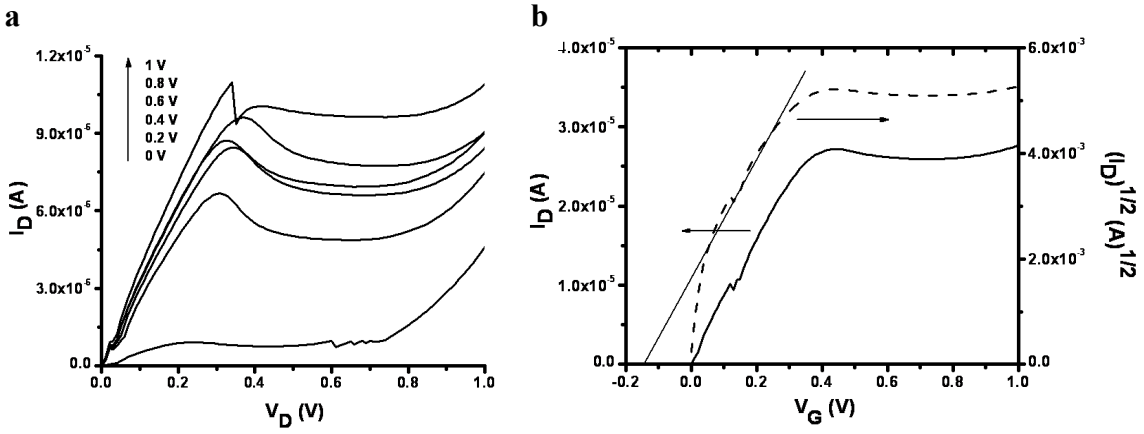

Fig. S16. Output (a) and Transfer (b) Characteristics of **2** with Hydrazine doping after 48hrs**.**

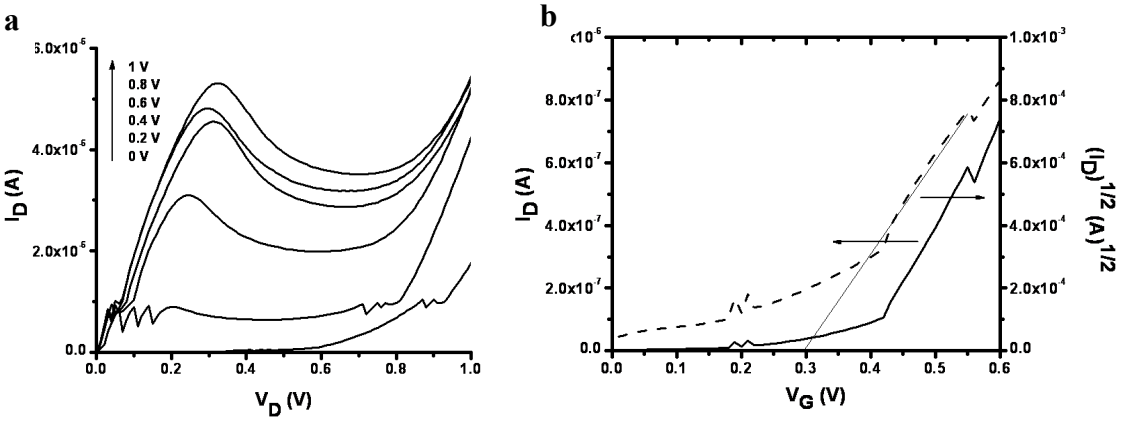

Fig. S17. Output (a) and Transfer (b) Characteristics of **2** with Hydrazine doping after 96hrs**.**

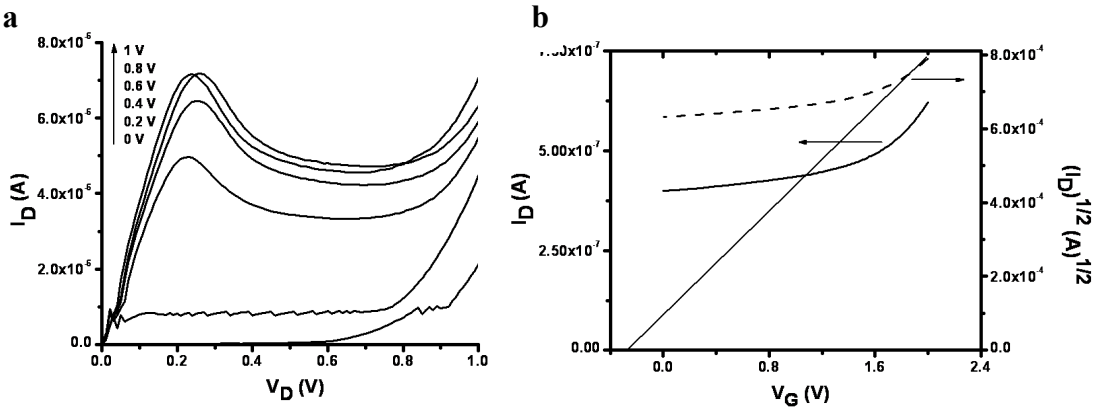

Fig. S18. Output (a) and Transfer (b) Characteristics of **2** with Hydrazine doping after 150hrs**.**

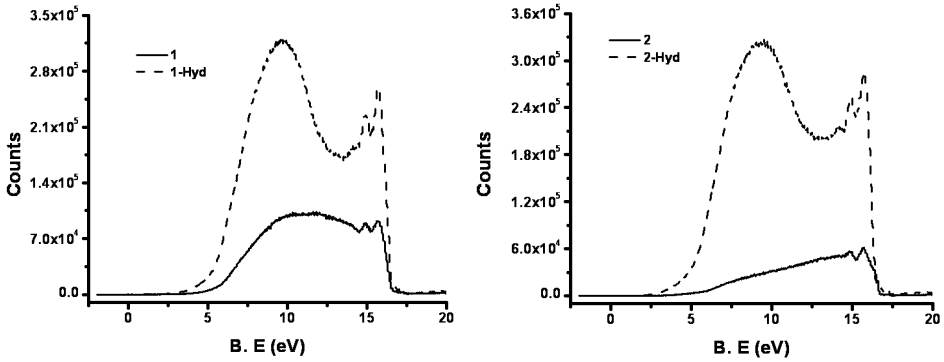

Fig. S19. *a)* UVPES spectra of compound **1** and b) **2** (with and without doping).

References:

1. P. K. Sukul, D. Asthana, P. Mukhopadhyay, D. Summa, L. Muccioli, C. Zannoni, D. Beljonne, A. E. Rowan, S. Malik, *Chem. Commun.* 2011, **47**, 11858.

2. S. Yang, X. Lin, A. Dailly, A. J. Blake, P. Hubberstey, N. R. Champness, M. Schröder, *Chem. Eur. J.* 2009, **15**, 4829.

3. A. Arulkashmir, R. Y. Mahale, S. S. Dharmapurikar, M. K. Jangid, K. Krishnamoorthy, *Polym. Chem.* 2012, **3**, 1641.

4. Y. Wang, H. Wang, Y. Liu, C. -A. Di, Y. Sun, W. Wu, G. Yu, D. Zhang, D. Zhu, *J. Am.Chem. Soc.* 2006, **128**, 13058.

5. K. Roy, C. P. Vinod, C.S. Gopinath, *J. Phys. Chem. C* 2013, **117**, 4717.

6. (a) S. G. Gholap, M. V. Badiger, C. S. Gopinath, J. Phys. Chem. B 2005, 109, 13941; (b) M. Logdlund, R. Lazzaroni, S. Stafstrom, W. R. Salaneck, J. -L. Brédas, Phys. Rev. Lett. 1989, 63, 1841; (c) J. H. Seo, T. -Q. Nguyen, J. Am. Chem. Soc. 2008, 130, 10042.

7. S. S. Dharmapurikar, A. Arulkashmir, C. Das, P. Muddellu, K. Krishnamoorthy, *ACS Appl. Mater. Interfaces*, 2013, 5, 7086.